Gfer inhibits Jab1-mediated degradation of $p27^{kip1}$ to restrict proliferation of hematopoietic stem cells

Ellen C. Teng[a], Lance R. Todd[b], Thomas J. Ribar[a], William Lento[a], Leah Dimascio[a], Anthony R. Means[a], and Uma Sankar[a,b,c]

[a]Department of Pharmacology and Cancer Biology, Duke University Medical Center, Durham, NC 27707; [b]James Graham Brown Cancer Center and Owensboro Cancer Research Program and [c]Department of Pharmacology and Toxicology, University of Louisville, Louisville, KY 42303

ABSTRACT **Growth factor erv1-like (Gfer) is an evolutionarily conserved sulfhydryl oxidase that is enriched in embryonic and adult stem cells and plays an essential prosurvival role in pluripotent embryonic stem cells. Here we show that knockdown (KD) of Gfer in hematopoietic stem cells (HSCs) compromises their in vivo engraftment potential and triggers a hyperproliferative response that leads to their exhaustion. KD of Gfer in HSCs does not elicit a significant alteration of mitochondrial morphology or loss of cell viability. However, these cells possess significantly reduced levels of the cyclin-dependent kinase inhibitor $p27^{kip1}$. In contrast, overexpression of Gfer in HSCs results in significantly elevated total and nuclear $p27^{kip1}$. KD of Gfer results in enhanced binding of $p27^{kip1}$ to its inhibitor, the COP9 signalosome subunit jun activation-domain binding protein 1 (Jab1), leading to its down-regulation. Conversely, overexpression of Gfer results in its enhanced binding to Jab1 and inhibition of the Jab1-$p27^{kip1}$ interaction. Furthermore, normalization of $p27^{kip1}$ in Gfer-KD HSCs rescues their in vitro proliferation deficits. Taken together, our data demonstrate the presence of a novel Gfer-Jab1-$p27^{kip1}$ pathway in HSCs that functions to restrict abnormal proliferation.**

Monitoring Editor
J. Silvio Gutkind
National Institutes of Health

Received: Aug 25, 2010
Revised: Feb 3, 2011
Accepted: Feb 16, 2011

INTRODUCTION

Hematopoietic stem cells (HSCs) are a largely quiescent population of cells that possess the ability to rapidly proliferate, self-renew, and differentiate into progenitors, thus ensuring the constant renewal of the billions of short-lived immune cells of the peripheral blood. During steady-state homeostasis, ~75% of long-term HSCs are in the G_0 phase of the cell cycle while the rest are asynchronously dividing, with the average cell-cycle doubling time being once in every 4–8 wk (Cheshier *et al.*, 1999). Another unique feature of HSCs is their ability to constantly switch between states of dormancy and activation, both during homeostasis and following periods of hematological stress (Wilson *et al.*, 2008). Whereas rapid proliferation in response to expansion cues and/or hematological stress is critical, abnormal HSC proliferation during homeostasis leads to compromised function (Cheng and Scadden, 2002; Kitsos *et al.*, 2005; Viatour *et al.*, 2008; Wilson *et al.*, 2008). Loss of quiescence often results in HSC exhaustion, underscoring the importance of tight regulation of proliferation by these cells (Orford and Scadden, 2008). Although various signaling pathways and cell-cycle inhibitors have been shown to regulate the capacity of HSCs to proliferate (Cheng et al., 2000a, 2000b; Park *et al.*, 2003; Ito *et al.*, 2004; Yilmaz *et al.*, 2006; Miyamoto *et al.*, 2007; Yalcin *et al.*, 2008), a comprehensive understanding of the mechanisms that execute the fundamental task of maintaining quiescence in these seminal cells is lacking.

Growth factor *erv1*-like (Gfer), the mammalian homologue of the yeast Erv1 protein, is a highly conserved FAD-dependent sulfhydryl oxidase (Lisowsky *et al.*, 2001). In yeast, *erv1* has roles in cytoplasmic Fe-S cluster assembly, mitochondrial biogenesis, and, along with its

This article was published online ahead of print in MBoC in Press (http://www.molbiolcell.org/cgi/doi/10.1091/mbc.E10-08-0723) on February 23, 2011.

Address correspondence to: Uma Sankar (uma.sankar@louisville.edu).

Abbreviations used: 7AAD, 1-amino actinomycin D; APC, allophycocyanin; BM, bone marrow; CDKI, cyclin-dependent kinase inhibitor; CML, chronic myeloid leukemia; CSN, COP9 signalosome; ESC, embryonic stem cell; Gfer, growth factor *erv1*-like; GFP, green fluorescent protein; HBSS, Hank's balanced salt solution; HSCs, hematopoietic stem cells; IMS, intermembrane space; IP, immunoprecipitation; IRES, internal ribosome entry site; Jab1, jun activation binding protein 1; KD, knockdown; KLS, $cKit^+Sca1^+Flk2^-CD34^-Lineage^-$; MSCV, murine stem cell virus; MSCV-C, MSCV control; PBS, phosphate-buffered saline; PE, phycoerythrin; PI, propidium iodide; R6G, rhodamine 6G; ROS, reactive oxygen species; SCF, stem cell factor; shRNA, short hairpin RNA; TEM, transmission electron microscopy; WT, wild type; YFP, yellow fluorescent protein.

© 2011 Teng *et al*. This article is distributed by The American Society for Cell Biology under license from the author(s). Two months after publication it is available to the public under an Attribution–Noncommercial–Share Alike 3.0 Unported Creative Commons License (http://creativecommons.org/licenses/by-nc-sa/3.0).

"ASCB®," "The American Society for Cell Biology®," and "Molecular Biology of the Cell®" are registered trademarks of The American Society of Cell Biology.

partner Mia-40, it forms a critical disulfide redox system instrumental in the import of small proteins, such as cytochrome *c* into the mitochondrial intermembrane space (IMS) (Becher *et al.*, 1999; Lange *et al.*, 2001; Lisowsky *et al.*, 2001; Mesecke *et al.*, 2005). In higher eukaryotes, Gfer and its homologues play roles in tissue regeneration (Klissenbauer *et al.*, 2002; Klebes *et al.*, 2005; Gatzidou *et al.*, 2006). Gfer maps within the stem cell–rich t-haplotype region of mouse chromosome 17 and is highly enriched in embryonic and adult stem cells (Polimeno *et al.*, 1999; Ivanova *et al.*, 2002; Ramalho-Santos *et al.*, 2002). In pluripotent mouse embryonic stem cells (ESCs), Gfer plays a specific, prosurvival role by regulating mitochondrial fission–fusion balance through its modulation of the key fission GTPase, Drp1 (Todd *et al.*, 2010a, 2010b). In multipotent HSCs, quantitative trait loci mapping studies aimed at uncovering regulatory pathways that affect cell function predicted Gfer to be important in proliferation and cell turnover (Bystrykh *et al.*, 2005). Its involvement in HSC proliferation and/or function, however, has yet to be verified.

We used gene knockdown (KD) and overexpression approaches to evaluate the precise role of Gfer in murine HSCs. We report herein that short hairpin (sh) RNA-mediated KD of Gfer in $cKit^+Sca1^+Flk2^-CD34^-Lineage^-$ (KLS) cells (a population that include HSCs) compromises their ability to successfully engraft the bone marrow of lethally irradiated recipient mice. Although Gfer KD in KLS cells did not affect cell survival, it did result in an unexpected, enhanced proliferation response in vitro that was followed by exhaustion. Whereas KD of Gfer in KLS cells significantly reduced $p27^{kip1}$, overexpression of Gfer enhanced the total and nuclear levels of this cell-cycle inhibitor. Further investigations of hematopoietic progenitor erythroid, myeloid and B-lymphoid (EML) cells revealed that Gfer interferes with the binding of $p27^{kip1}$ with its inhibitor jun activation binding protein 1 (Jab1), thus enhancing nuclear retention and/or stability of this cyclin-dependent kinase inhibitor (CDKI). Furthermore, restoration of normal $p27^{kip1}$ levels in Gfer-KD KLS cells resulted in restoration of normal proliferation in vitro. Thus, our cumulative results support a role for Gfer in the restriction of unwarranted HSC proliferation through its inhibition of Jab1-mediated turnover of $p27^{kip1}$.

RESULTS

KD of Gfer expression in KLS cells significantly impairs in vivo function

To evaluate the biological function of Gfer in HSCs, we knocked down Gfer using a previously reported FG12-Lentivirus–green fluorescent protein (GFP)–shRNA system (Qin *et al.*, 2003; Todd *et al.*, 2010a). KLS cells freshly isolated from wild-type (WT) mice were infected with Lenti-shRNA-GFP viruses containing Gfer1 (Gfer1-KD; targeting exon 2); Gfer2 (Gfer2-KD; targeting the 3′ untranslated region) and/or nonspecific LacZ (LacZ-KD) shRNAs. Uninfected WT KLS cells (WT-U), cultured similarly to the virus-infected cells, served as controls in these experiments. Approximately 72 h later, viable GFP^- (WT-U) or GFP^+ virus-infected (LacZ-KD and Gfer-KD) KLS cells were reisolated and evaluated for Gfer expression. We achieved ~72 and 57% KD of Gfer mRNA and protein using Gfer1 and 2 shRNAs, respectively (Figure 1, A and B).

To investigate whether down-regulation of Gfer in KLS cells affected their in vivo function, we performed competitive bone marrow (BM) transplantation by transplanting ~10,000 CD45.2 WT-LacZ-KD, WT-Gfer-KD, and WT-U KLS cells along with 300,000 competing CD45.1 total bone marrow cells into cohorts of eight lethally irradiated CD45.1 recipient mice. We analyzed bone marrow cells from recipient mice 48 h after the transplant and confirmed that CD45.2-donor-derived cells from all genetic backgrounds "homed" to the bone marrow of host mice (Supplemental Figure 1A). Flow cytometric analysis of peripheral blood from transplant recipients revealed that, whereas WT-U and WT-LacZ KLS cells reconstituted at similar rates, achieving an average of 45% donor chimerism by 3 wk and 90% by 15 wk after BM transplantation, KD of Gfer resulted in a significant reduction in reconstitution, with an average of 8–13% CD45.2 donor reconstitution during the 19-wk period (Figure 1, Ci and Cii). Analysis of recipient bone marrow at the end of the 19-wk BM transplantation period revealed that an average of 2.3% of LacZ-KD $CD45.2^+$ KLS cells and 0.2% of Gfer-KD $CD45.2^+$ KLS cells (Supplemental Figure 1B) remained in the recipient bone marrow, indicating that the fundamental defect of engraftment following KD of Gfer occurred in the KLS cells. To verify whether the remaining $CD45.2^+$ Gfer-KD cells in transplant recipients represented "escapers" from KD, we isolated CD45.2 $Lineage^{Negative}$ cells from transplant recipients at week 15 and measured the levels of Gfer mRNA. As shown in Supplemental Figure 1C, Gfer mRNA was still expressed twofold lower in $CD45.2^+$ $Lineage^{Negative}$ Gfer-KD than in LacZ-KD cells, indicating that the shRNA was still active in these cells. Collectively these data support a role for Gfer in the maintenance of HSC function in vivo.

Diminished Gfer in KLS cells triggers enhanced proliferation followed by exhaustion

Down-regulation of Gfer in the ESCs triggers apoptosis accompanied by a loss of mitochondrial function (Todd *et al.*, 2010a). To understand whether KD of Gfer triggers apoptosis in KLS cells, we analyzed LacZ and Gfer-KD KLS cells (freshly resorted 72 h after virus infection) for annexin V/7-amino actinomycin D (7AAD) reactivity by flow cytometry. As indicated in Figure 2A, down-regulation of Gfer did not result in a significant loss of cell viability through apoptosis. We further examined the mitochondrial morphology in LacZ and Gfer-KD KLS cells by transmission electron microscopy (TEM). LacZ-KD KLS cells possessed an average of 6–10, round to oval, mitochondria with well-defined cristae. In contrast, whereas the majority of Gfer-KD mitochondria appeared swollen with intact overall morphology, the remaining mitochondria in these cells appeared to be in various stages of degeneration (Figure 2B). Down-regulation of Gfer, however, did not result in a significant loss of mitochondrial function (unpublished data). Overall these results indicate that KD of Gfer resulted in alteration of mitochondrial morphology without compromising overall cell survival.

Next we evaluated whether down-regulation of Gfer in KLS cells affected their ability to proliferate. To this end, equal numbers of LacZ, Gfer1, and Gfer2 KD KLS cells were grown in vitro in serum-free medium containing stem cell factor (SCF) and Flt3 ligand for 8 d. Comparison of the KLS profiles of these cells at days 0 and 6 of the in vitro proliferation assay revealed that differentiation occurred at a similar rate in LacZ and Gfer KD cells (Supplemental Figure 2A). Surprisingly, down-regulation of Gfer expression resulted in significantly enhanced proliferation in vitro, such that by day 4, there were twice as many Gfer-KD as there were LacZ-KD cells (Figure 2C). Furthermore, by day 6, there were 2- to 2.5-fold higher numbers of Gfer KD than LacZ-KD cells in culture, respectively (Figure 2C). In contrast, by day 8, the majority of the Gfer1/2-KD cells underwent exhaustion (Figure 2C and Supplemental Figure 2B). We additionally verified that down-regulation of Gfer was similar in Gfer-KD cells at days 0 and 6 in culture (unpublished data). Increased proliferation followed by loss of function has been observed in *ataxia-telangiectasia mutated* ($Atm^{-/-}$) and $Foxo3a^{-/-}$ HSCs, where diminished quiescence is accompanied by elevated reactive oxygen species (ROS) (Ito *et al.*, 2006; Miyamoto *et al.*, 2007). To evaluate whether

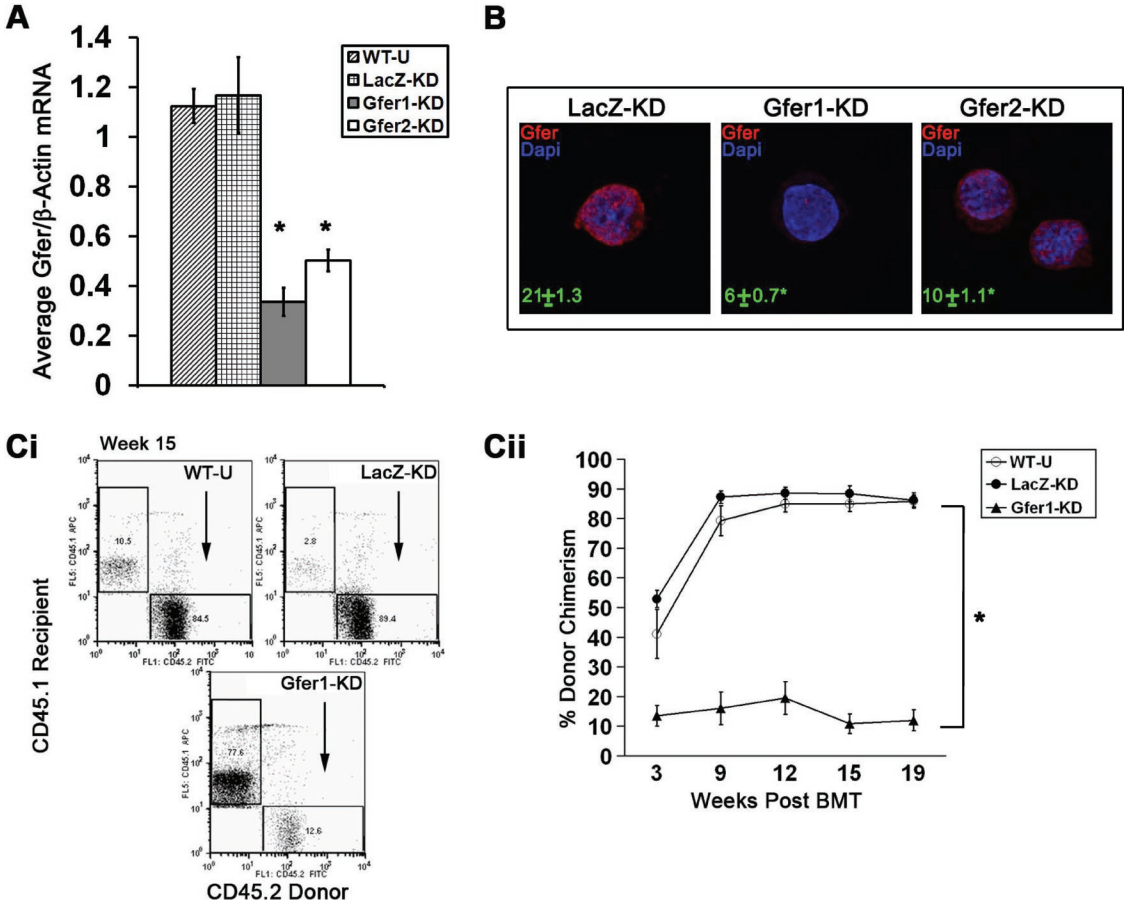

FIGURE 1: Gfer is a novel regulator of HSC function. (A) Average Gfer mRNA, normalized to those of β-actin, from uninfected (U) WT (WT-U), LacZ-KD, and Gfer-1/2KD KLS cells, measured by quantitative RT-PCR at 72 h after viral infection. Error bars represent SD of the average values (n = 4); *p < 0.05. (B) Digital optically sectioned immunocytochemistry images (630×) depicting Gfer protein levels in red and DAPI in blue from LacZ-KD and Gfer-1/2KD KLS cells at 72 h after viral infection. Average signal intensities ± SD from ~150 cells (n = 3) are shown in green. (Ci) Representative histograms showing engraftment in individual recipients by CD45.2 donor cells (*x*-axis) at 15 wk after BM transplantation. We used eight recipient mice per donor cell genotypes per experiment (n = 3). (Cii) Line graph depicting average CD45.2 donor reconstitution by the indicated donor genotype at 3, 9, 12, 15, and 19 wk after BM transplantation. Donor reconstitution by uninfected WT donor cells is also shown. Error bars represent SEM of reconstitution by individual recipients (n = 8) within each group; *p < 0.05.

an increase in oxidative stress in Gfer-KD cells triggers a hyperproliferative response, we measured ROS levels in LacZ- and Gfer-KD cells on days 6 and 8 of growth in culture using the redox-active fluorescent probe dihydrorhodamine 6G (dihydro-R6G) by flow cytometry. We did not observe significant differences in R6G fluorescence intensities between LacZ- and Gfer-KD cells on days 6 and 8 of proliferation in vitro (Figure 2D), indicating that the enhanced proliferation in Gfer-KD cells is not due to oxidative stress.

Gfer modulates total and nuclear levels of $p27^{kip1}$ in KLS cells

Our data suggest that KD of Gfer from KLS cells triggers enhanced cell proliferation that results in exhaustion and loss of in vivo function, but what might be the mechanism that elicits a hyperproliferative response in Gfer-KD KLS cells? Gfer directly interacts and colocalizes in the nucleus with Jab1, the 5th subunit of the highly conserved COP9 signalosome (CSN) protein complex (Lu *et al.*, 2002; Wang *et al.*, 2004). The CSN complex consists of a multisubunit protease that functions in the ubiquitin–proteasome pathway by directly regulating the activities of the cullin–RING ligase family of ubiquitin E3 complexes (Wei *et al.*, 2008; Kato and Yoneda-Kato, 2009; Schwechheimer and Isono, 2010). Jab1 binds to the cell-cycle inhibitor $p27^{kip1}$ through its C-terminal domain, coordinating nuclear export and subsequent proteasome-dependent degradation of this CDKI (Tomoda *et al.*, 1999, 2002); and Jab1 is expressed in HSCs (Mori *et al.*, 2008).

We hypothesized that, in normal KLS cells, Gfer binds to and inactivates Jab1, resulting in stabilization of $p27^{kip}$ and cell quiescence. To test this hypothesis, we first assessed $p27^{kip1}$ and Jab1 protein levels in LacZ and Gfer-KD KLS cells by fluorescence immunocytochemistry. Down-regulation of Gfer (Figure 3, vii and viii) resulted in a significant twofold reduction in overall (total and nuclear) $p27^{kip1}$ levels (Figure 3, i and ii), without significant alterations in Jab1 levels (Figure 3, iv and v; Supplemental Figure 3A). Furthermore, treatment of Gfer-KD KLS cells with the proteasome inhibitor MG132 resulted in significantly increased nuclear and total $p27^{kip1}$ levels, consistent with its increased turnover in the absence of Gfer (Supplemental Figure 3B, i–iv). We then asked whether $p27^{kip1}$ and Jab1 levels were altered in KLS cells overexpressing Gfer. Murine stem cell virus (MSCV)-mediated overexpression of Gfer (Figure 3ix)

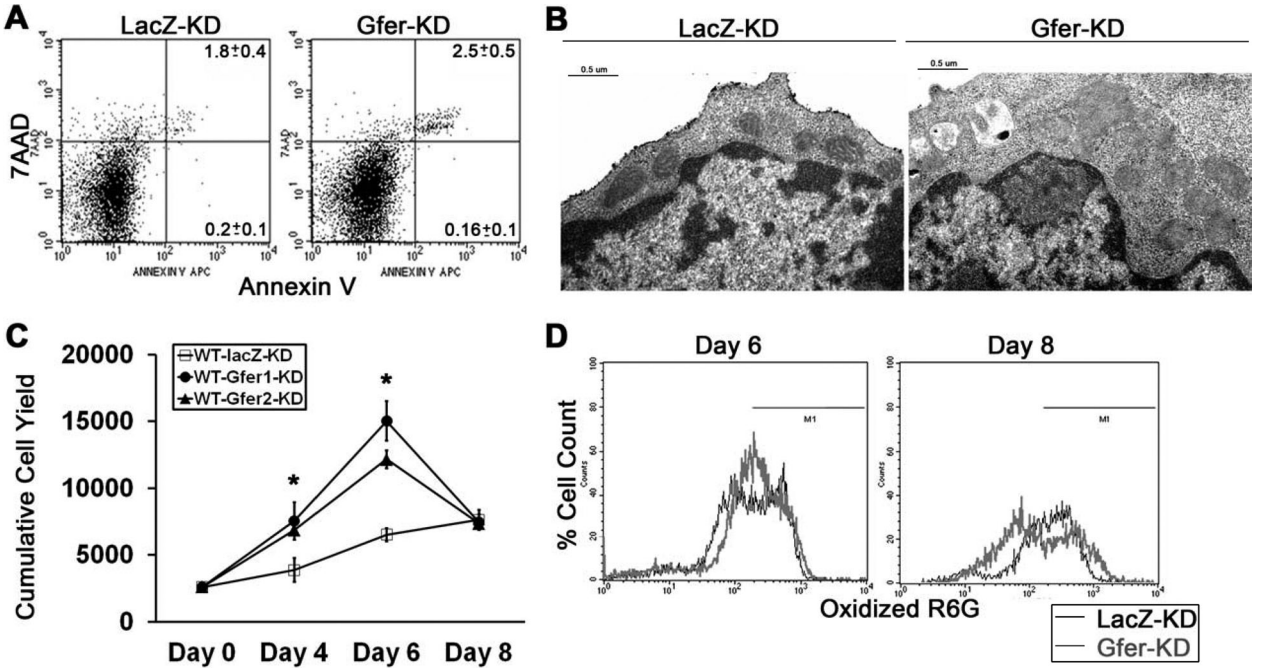

FIGURE 2: KD of Gfer in KLS cells results in enhanced proliferative capacity. (A) Apoptosis assessed in resorted GFP$^+$ LacZ and Gfer-KD KLS cells by measuring Annexin V and 7AAD reactivity. Representative histograms with average percentage of early and late apoptotic cells ± SD from n = 3 experiments are shown; p = 0.3. (B) TEM images, 25,000× magnifications, depicting the ultrastructural details in LacZ and Gfer-KD KLS cells. Scale bars represent 0.5 μm. (C) Average (n = 3) cumulative cell yield from indicated genotypes during in vitro proliferation assays performed in Terasaki plates for 8 d in serum-free medium; *p < 0.05. (D) Representative histograms (n = 2) indicating intracellular ROS levels in LacZ and Gfer KD KLS cells on days 6 and 8 of the proliferation assay. Measurements were based on the production of oxidized R6G by the intracellular oxidation of the nonfluorescent dihydro-R6G. The percentage of cells (*y*-axis) and oxidized R6G fluorescence intensities (*x*-axis) in Lacz and Gfer KD KLS cells are shown.

resulted in a significant 1.6-fold increase in p27^{kip1}, 85% of which was retained in the nucleus (Figure 3iii), whereas total Jab1 protein levels did not change (Figure 3vi). Conversely, levels of p21^{cip1}, a member of the cip/kip-cell cycle inhibitor family with demonstrated roles in HSC quiescence (Cheng *et al*., 2000b), did not change when Gfer was down-regulated or overexpressed (Supplemental Figure 4). Altogether these results indicate that Gfer expression significantly modulates total and nuclear p27^{kip1} in KLS cells.

Gfer binds to Jab1 and inhibits its destabilization of p27^{kip1}

Testing the hypothesis that Gfer regulates p27^{kip1} levels via its interaction with Jab1 would require traditional biochemical techniques, such as immunoprecipitation (IP) followed by SDS–PAGE and immunoblot analyses of the precipitates. Such tasks, however, are impractical to accomplish in HSCs because of their rarity. HSCs constitute only 0.01% of total bone marrow, amounting to an approximate yield of 10,000 cells per mouse. Moreover, being small (average diameter of 4 μm), and largely quiescent, HSCs possess a limited amount of protein (Viatour *et al*., 2008; Wilson *et al*., 2008). Hence we turned to the hematopoietic progenitor EML1 cell line (Tsai *et al*., 1994) to study the mechanism of regulation of p27^{kip1} stability by Gfer. First, we performed KD and overexpression of Gfer in EML cells using the previously mentioned FG12 Lentivirus and MSCV systems (Figure 4, Ai and Aii). Overexpression of Gfer increased p27^{kip1}, and its KD decreased the levels of the CDKI, without a significant alteration of Jab1 levels (Figure 4, Ai and Aii). We then analyzed Jab1-IP complexes from these EML cells for the presence of Gfer and p27^{kip1}. As shown in Figure 4, Bi and Bii, endogenous Gfer bound to Jab1 in MSCV control (MSCV-C) and FG12 LacZ-infected EML cells; this interaction was enhanced on Gfer overexpression and diminished on Gfer KD. In contrast, the amount of p27^{kip1} present in Jab1-IP complexes decreased in MSCV-Gfer–infected EML cells and increased in Gfer-KD cells (Figure 4, Bi and Bii). Similarly, there was a marked reduction of Jab1 in p27^{kip1}-IP complexes from MSCV-Gfer compared with MSCV-C cells and an increase in Jab1 present in these complexes in Gfer-KD compared with the nonspecific LacZ-KD EML cells (Figure 4, Ci and Cii). Furthermore, ubiquitination in p27^{kip1}–IP complexes was significantly higher in Gfer-KD EML cells, whereas it was almost abolished in p27^{kip1} immunocomplexes from cells overexpressing Gfer (Figure 4, Ci and Cii; Zhou *et al*., 2009). Thus, raising the concentration of Gfer resulted in sequestration of Jab1, leaving less of this CSN subunit available for association with p27^{kip1} and orchestration of its nuclear export and degradation.

Normalization of p27^{kip1} levels rescues the enhanced proliferation deficit in Gfer-KD KLS cells

We next determined whether expression of p27^{kip1} in Gfer-KD KLS cells would rescue their in vitro proliferation defects by using a modified MSCV–internal ribosome entry site (IRES)–yellow fluorescent protein (YFP) to achieve restoration, but not overexpression, of p27^{kip1} in these cells (Supplemental Figure 3, Bi, iii, and iv for p27^{kip1} protein and 3Bvi for p27^{kip1} mRNA). We also confirmed that infection of Gfer-KD KLS cells with MSCV-p27^{kip1}-YFP did not cause enhanced differentiation and/or apoptosis (unpublished data). Normalization of p27^{kip1} levels in Gfer-KD KLS cells to those found in control cells resulted in a rescue of the enhanced proliferation deficit in the mutant cells (Figure 5A). Moreover, Gfer-KD KLS cells

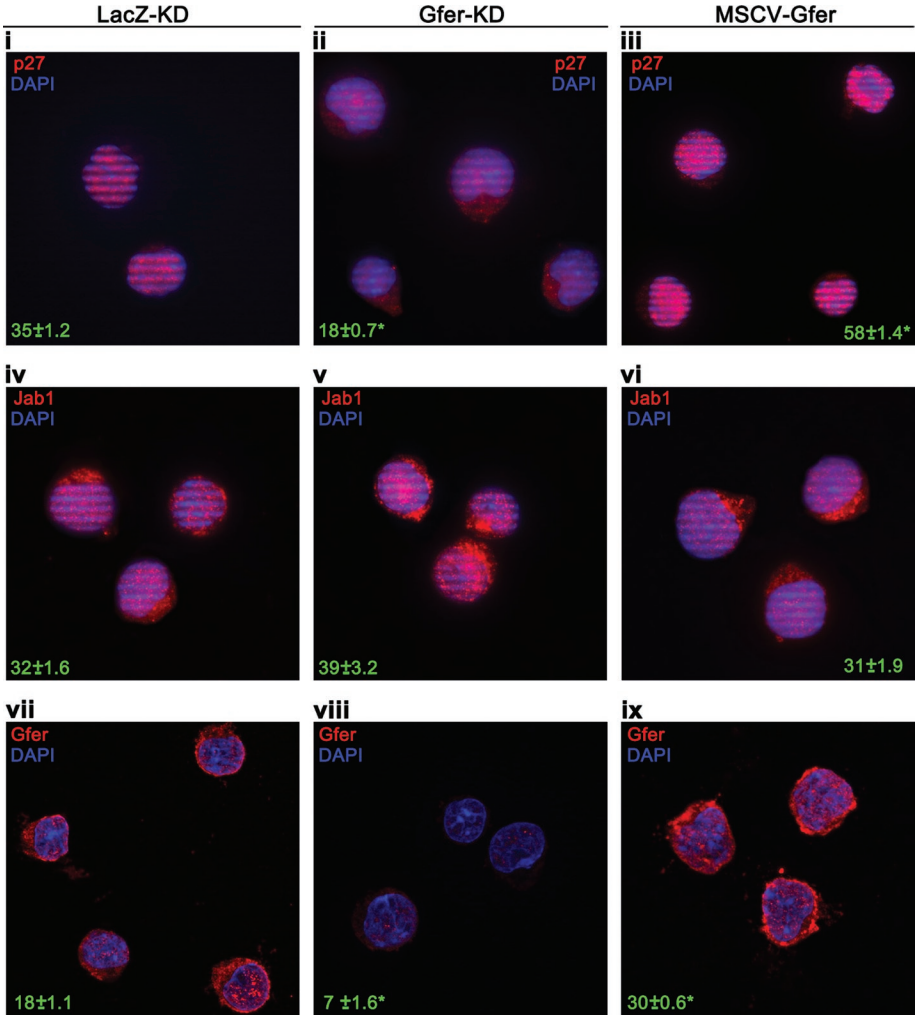

FIGURE 3: Gfer expression modulates total and nuclear p27^{kip1} in KLS cells. Digital optical section (Apotome; 630×) immunocytochemistry images depicting p27^{kip1} (i–iii), Jab1 (iv–vi), and Gfer (vii–ix) levels in LacZ and Gfer KD and MSCV-Gfer KLS cells. Protein levels were detected by probing with secondary antibodies conjugated to Cy3 (red) fluorophore. DAPI is shown in blue, and average signal intensities ± SD calculated from at least 250 cells from five independent experiments are indicated in green. *$p < 0.05$.

expressing MSCV-p27^{kip1}-YFP did not undergo exhaustion by day 8 of the proliferation assay, suggesting that enhanced proliferation by the mutant cells may have caused their exhaustion and, perhaps, loss of in vivo function. Furthermore, whereas overexpression of Gfer did not alter the in vitro doubling time of KLS cells (Figure 5A), it did cause increased differentiation (Supplemental Figure 5A). Furthermore, MSCV-Gfer KLS cells possessed enlarged, mostly round or oval, mitochondria (Supplemental Figure 5B), indicating that the altered mitochondrial morphology may partially contribute to the enhanced differentiation of these cells (Mantel *et al.*, 2010). Nevertheless, our cumulative data suggest that, in normal HSCs, Gfer acts to counter Jab1-mediated nuclear export and destabilization of the CDKI p27^{kip1}, by directly binding to and sequestering the CSN subunit (Figure 5B). Through this mechanism, Gfer promotes quiescence in HSCs, thus playing a critical role in maintaining the functional integrity of these important cells.

DISCUSSION

HSC quiescence, tightly regulated by various intrinsic and extrinsic mechanisms, ensures the maintenance of long-term genetic, epigenetic, and mitochondrial stability (Wilson and Trumpp, 2006). Consequently, loss of quiescence in long-term repopulating HSCs results in their exhaustion and/or loss of function. Genes that execute the fundamental task of restricting unwarranted HSC proliferation thus play important roles in the maintenance of their function during homeostasis and periods of hematological stress. In this study, we show that the highly conserved sulfhydryl oxidase Gfer performs a novel, fundamental role in the restriction of HSC proliferation through its modulation of Jab1-mediated turnover of the key cell-cycle inhibitor, p27^{kip1}. KD of Gfer from KLS cells results in a loss of cell quiescence and in vivo function. Gfer-KD cells display reduced p27^{kip1} levels, whereas its overexpression significantly elevates p27^{kip1} levels and enhances its nuclear retention. In hematopoietic EML cells, Gfer binds to the CSN subunit Jab1, preventing its association with p27^{kip1}, thereby inhibiting Jab1-mediated nuclear export and increased turnover of this CDKI. Accordingly, restoration of p27^{kip1} in KLS cells down-regulated for Gfer expression normalizes their in vitro proliferation kinetics, indicating a proquiescence role for the novel Gfer-Jab1-p27^{kip1} pathway in HSCs. Indeed, decreased p27^{kip1} correlates with the loss of HSC quiescence in *Foxo3a*$^{-/-}$ mice, underscoring a role for this CDKI in regulating HSC proliferation (Miyamoto *et al.*, 2007). Unlike Gfer-KD KLS cells, however, HSCs from p27^{kip1}-null mice did not undergo abnormal proliferation (Cheng *et al.*, 2000a). Enhanced p21^{cip1} levels restricted unwanted proliferation in p27^{kip1}-null HSCs, whereas the levels of p21^{cip1} did not increase in Gfer-KD KLS cells. In contrast, this discrepancy could be due to genetic differences, as our HSCs were derived from C57BL/6 mice, whereas the p27^{kip1}-null mice were generated in the SV129 background.

Besides its predominant localization in the IMS of mitochondria, Gfer is also present in the cytoplasm and nucleus; and a nonmitochondrial activity is associated with its role in spermatogenesis (Klissenbauer *et al.*, 2002). The mitochondrial morphology in KLS cells down-regulated for or overexpressing Gfer was not nearly as dramatic as that observed in ESCs. We also did not observe loss of mitochondrial membrane potential, elevation of intracellular ROS, or decrease in cell viability in Gfer-KD KLS cells. Our data strongly suggest that the nuclear function of Gfer, inhibiting Jab1 and stabilizing p27^{kip1} to restrict proliferation, is the most important one in HSCs. In fact, Gfer binds Jab1 through its divergent N-terminal domain, as opposed to the highly conserved FAD domain (Wang *et al.*, 2004). In contrast, in ESCs, the mitochondrial function of Gfer is the most relevant as its down-regulation resulted in extensive mitochondrial fragmentation and apoptosis (Todd *et al.*, 2010a), indicating that the role of Gfer in maintaining mitochondrial integrity may be associated with the more primitive status of the ESCs. Furthermore, Gfer is largely dispensable for maintenance of mitochondrial

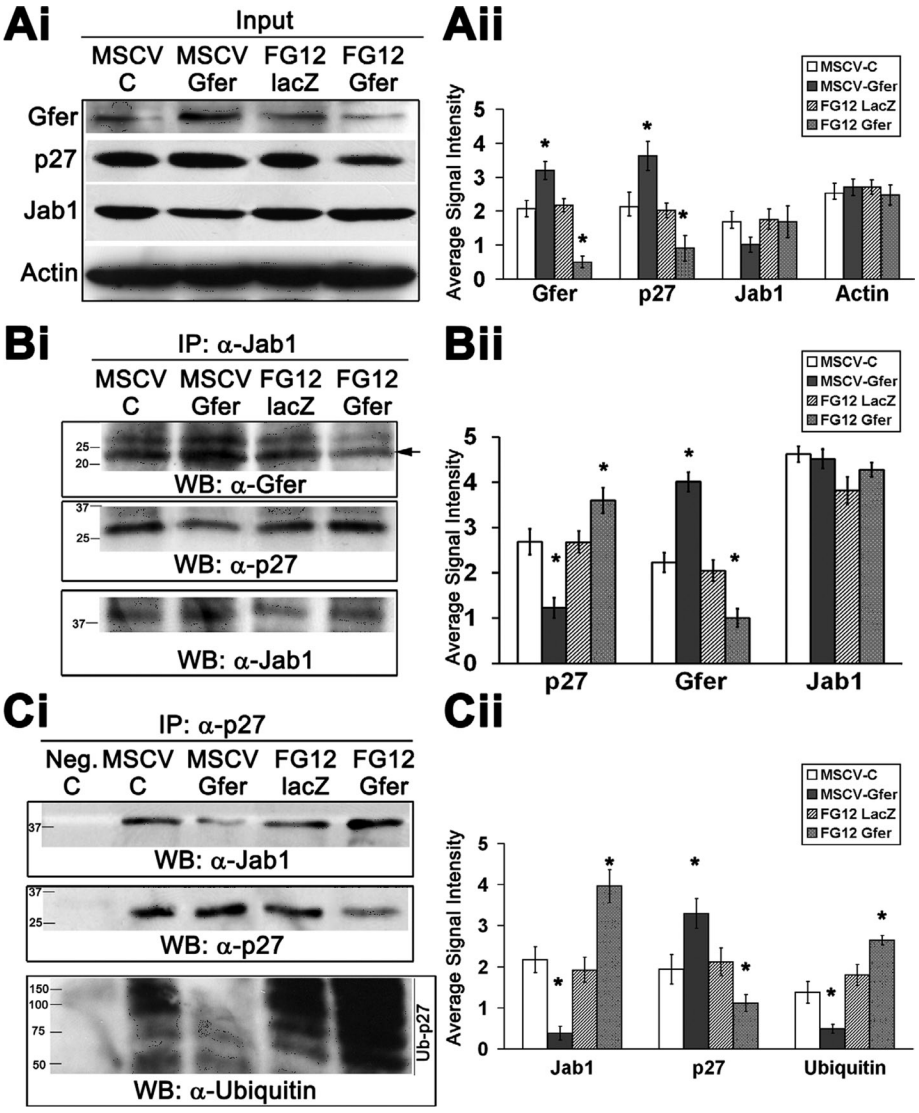

FIGURE 4: Gfer regulates the stability of p27^{kip1} through its interaction with Jab1. (Ai) Immunoblots showing Gfer, p27^{kip1}, Jab1, and actin (loading control) levels in whole-cell lysates from MSCV-C–, MSCV-Gfer–, FG12 LacZ–, and FG12 Gfer–infected EML hematopoietic progenitor cells. (Aii) Average signal intensities of bands from corresponding immunoblots of the indicated genotypes from n = 3 experiments; *p < 0.05. (Bi) Immunoblots depicting the levels of Gfer, p27^{kip1}, and Jab1 present in anti-Jab1 immunoprecipitates from EML cells of the indicated genotypes. Black arrow indicates Gfer (23 kDa). (Bii) Average signal intensities of bands showing Gfer, p27^{kip1}, and Jab1 levels in Jab1-IP complexes from three experiments; *p < 0.05. (Ci) Western blot images indicating the levels of Jab1, p27^{kip1}, and ubiquitin associated with anti-p27^{kip1} immunoprecipitates in control, Gfer-KD–, or Gfer-overexpressing EML cells. Negative control indicates a beads-only control with no primary antibody performed with MSCV-C EML cells. (Cii) Graphs showing average signal intensities of bands showing Jab1, p27^{kip1}, and ubiquitin levels in p27-IP complexes from three experiments; *p < 0.05.

function and cell survival in more differentiated cells (Todd *et al.*, 2010a).

The multifunctional Jab1 modulates the stability of a plethora of cell regulatory proteins. Although it stabilizes c-jun, hypoxia-inducible factor 1α subunit, and mdm-2, Jab1 also directly promotes the nuclear export of several key regulators of cellular homeostasis, including p53 and p27^{kip1} (Wei *et al.*, 2008; Kato and Yoneda-Kato, 2009; Schwechheimer and Isono, 2010). Highly elevated Jab1 and low or cytoplasmic p27^{kip1} are indicators of poor prognosis in multiple types of cancers, including chronic myeloid leukemia (CML) (Tomoda *et al.*, 2005). Transgenic expression of a stable form of Jab1 significantly enhanced the proliferative potential of hematopoietic progenitors in mouse bone marrow (Mori *et al.*, 2008). Our data indicating a direct interaction of Gfer with Jab1 to restrict Jab1-mediated destabilization of p27^{kip1} (Figure 5B) underscores the importance of a Gfer-Jab1-p27^{kip1} pathway not only in the functional maintenance of normal HSCs, but also in the prevention and/or treatment of malignancies. Controlled modulation of Gfer expression to inhibit Jab1 and thereby elevate p27^{kip1} could be a relevant therapeutic strategy in the treatment of CML and other myeloproliferative diseases.

MATERIALS AND METHODS

Mice

C57BL/6 (CD45.2) and B6.SJL-Ptprc^{a} Pep3^{b}/BoyJ (CD45.1) strains of mice were purchased from The Jackson Laboratory (Bar Harbor, ME) or Taconic Farms (Hudson, NY). All animals were housed in the Levine Science Research Center Animal Facility located at Duke University or in the University of Louisville Baxter II Vivarium under a 12-h light, 12-h dark cycle. Food and water were provided ad libitum. All care and experimental procedures were performed according to Duke University and University of Louisville Institutional Animal Care and Use Committee protocols and in compliance with National Institutes of Health guidelines on the use of laboratory and experimental animals.

Isolation of KLS cells

Isolation of KLS cells from BM cells was performed as described previously (Morrison *et al.*, 1997; DiMascio *et al.*, 2007). Briefly, BM cells devoid of red blood cells were first enriched for c-Kit by staining with CD117 antiboby–conjugated microbeads (Miltenyi Biotech, Bergisch Gladbach, Germany) followed by positive selection. The cKit-enriched BM cells were further stained with propidium iodide (PI) and an antibody cocktail containing allophycocyanin (APC)-conjugated c-Kit (2B8), phycoerythrin (PE)-Cy5–conjugated Sca-1 (D7), and PE-conjugated lineage markers, including CD3e (145–2C11), CD4 (GK1.5), CD5 (53.7.8), CD8 (53.6.7), B220 or CD45R (6B2), Ter119 or Ly76, Mac1 or CD11b (M1/70), Gr1 (RB6–8C5), CD16/32 or FCγR Block (93), Flk2/Flt3/Ly72 (A2F100), and CD34 (RAM34) (all obtained from eBioscience, San Diego, CA). Viable (PI^{neg}) KLS cells that include long- and short-term HSCs were sorted using a fluorescence-activated cell sorting (FACS) analysis (FACSVantage or FACSAria; BD Biosciences, San Jose, CA).

Virus production and infection of HSCs

FG12-Lenti-GFP-shRNA Gfer1/2 and LacZ viruses were produced as previously described using 293T cells (Qin *et al.*, 2003; Todd *et al.*,

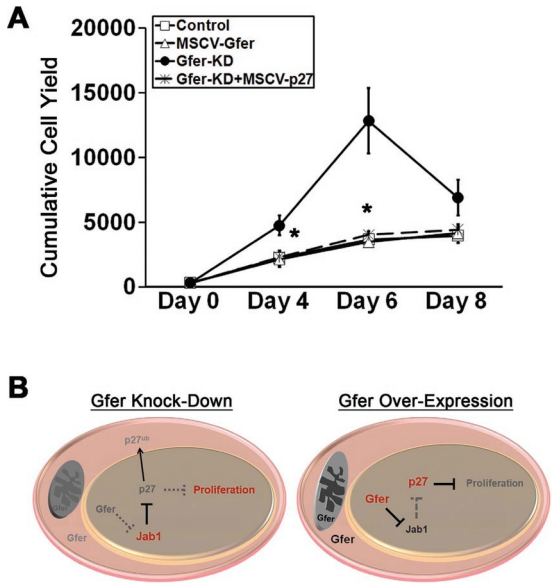

FIGURE 5: Normalization of $p27^{kip1}$ levels in Gfer KD KLS cells rescues their proliferation/exhaustion defect. (A) Average cumulative cell yield (n = 3) from control, MSCV-Gfer, and Gfer-KD KLS cells and in Gfer-KD KLS cells expressing MSCV-$p27^{kip1}$-YFP virus. Cumulative cell yield was calculated by counting the total number of cells per well of Terasaki plates initially plated with KLS cells of the indicated genotypes cultured on serum-free medium containing SCF and Flt3 ligand; *$p < 0.05$. (B) Model proposing a novel role for Gfer in the restriction of unwarranted HSC proliferation through its inhibition of Jab1-mediated ubiquitination and turnover of $p27^{kip1}$. Down-regulation of Gfer in KLS cells results in its inability to efficiently inhibit Jab1 from binding to and causing the nuclear export and subsequent degradation of $p27^{kip1}$. Degradation of this CDKI results in increased proliferation of HSCs during homeostasis, resulting in their eventual exhaustion and loss of in vivo function. In contrast, increased concentration of Gfer in KLS cells results in its increased binding and sequestering of Jab1, leading to increased nuclear retention and stability of $p27^{kip1}$, which then blocks the ability of G1 cyclin-Cdk complexes to organize the progression of the cell cycle.

2010a). Mouse *Gfer* and $p27^{kip1}$ cDNA constructs were obtained from Open Biosystems (Huntsville, AL), PCR amplified, and cloned into MSCV–IRES–GFP or MSCV—IRES–YFP vectors. Retrovirus production was performed as previously described (Kitsos *et al.*, 2005). Approximately 30,000 freshly isolated KLS cells were sorted per well into a 96-well, U-bottom plate (BD Biosciences) in the presence of X-vivo-15 (Cambrex, Walkersville, MD) medium supplemented with 2% fetal bovine serum, 30 ng/ml SCF, 30 ng/ml Flt-3 ligand, and 50 μM 2-mercaptoethanol. The cells were then infected with the appropriate Lenti- or retroviruses at a multiplicity of infection (MOI) of 5:1 along with 4 μg/ml Polybrene (Sigma Aldrich, St. Louis, MO). Viable (PI^{neg}) GFP- and/or YFP-positive cells that were also positive for cKit and Sca1 and negative for Lineage markers (GFP/YFP^+KLS) were resorted for appropriate experiments after 72 h of infection (see Supplemental Figure 2A, left panel). Uninfected control cells were cultured for 72 h as well and sorted for positive expression of cKit and Sca1 and negative for Lineage markers.

In vivo HSC functional assays

Congenic CD45.1 mouse strains B6.SJL-$Ptprc^a$-$Pep3^b$/BoyJ (The Jackson Laboratory) or B6.SJL-*Ptprc*^{a}/BoyAiTac (Taconic Farms) were lethally irradiated with 9.5 Gy using a cesium irradiator 24 h before the transplant. We used six to eight recipient mice per sample genotype. Uninfected KLS cells or GFP^+-Lenti-Gfer or LacZ shRNA virus-infected KLS cells were FACS resorted, as mentioned earlier in the text, after 72 h in culture. Approximately 10,000 donor cells (all CD45.2) were retro-orbitally injected into groups of 8 recipient mice along with 300,000 rescuing CD45.1 Sca1-depleted total BM cells. We used a high number of donor cells (10,000) to initiate the transplant to ensure successful engraftment by GFP-Lentivirus–infected KLS cells. Transplant recipients were monitored daily and were maintained on antibiotic water. Mice that received transplants were bled at 3, 9, 12, 15, and 19 wk posttransplant to determine the percentage of chimerism and reconstitution. Donor and host cells were distinguished by allelic expression of CD45.2/CD45.1. At 15 wk posttransplant, $Lineage^-CD45.2^+$ cells from total BM pooled from three transplant recipients in each class were isolated for analysis of Gfer mRNA levels.

In vitro proliferation assays of KLS cells

GFP^+ Lenti-shRNA virus– or GFP^+/YFP^+ MSCV–infected and/or GFP^- uninfected KLS cells were FACS sorted at 10 cells per well into Terasaki plates (BD Biosciences). The cells were grown in serum-free medium (Stem Cell Technologies, Vancouver, BC, Canada) supplemented with 90 ng/ml SCF, 30 ng/ml Flt-3 ligand (both from R&D Systems, Minneapolis, MN), 50 U/ml penicillin/streptomycin (Invitrogen, Carlsbad, CA), and 50 μM 2-mercaptoethanol (Millipore, Billerica, MA) for 8 d. Proliferation rate of the plated cells was estimated by counting the number of cells in each well at 2, 4, 6, and 8 d of culture. On the 6th day of proliferation, cells from all wells of an extra Terasaki plate were pooled, stained for KLS antibodies, fixed in 1% paraformaldehyde (PFA; Polysciences, Warrington, PA), and analyzed for differentiation by flow cytometry.

Apoptosis assays

On days 0, 6, and 8 of in vitro culture, cells from all wells of an extra Terasaki plate were pooled. Staining for Annexin V/7-AAD on KLS cells was performed using the Annexin V-APC Apoptosis Detection Kit I (BD Biosciences), following the manufacturer's suggested protocol. Harvested cells were washed twice in cold phosphate-buffered saline (PBS) and suspended in 1× Annexin V Binding Buffer (part of the kit) at a concentration of 1×10^6 cells/ml. Samples were then analyzed within 1 h by flow cytometry using BD FACSVantage (BD Biosciences).

ROS detection assays

On days 0, 6, and 8 of in vitro culture, cells originally plated at a density of 5000 cells per well in a 96-well plate were harvested and loaded with 5 μM dihydro-R6G (Molecular Probes, Invitrogen) in Hank's balanced salt solution (HBSS) for 45 min under normal growth conditions. Cells were then washed, resuspended in fresh HBSS, and analyzed by flow cytometry using BD FACScan. Intracellular oxidation of this nonfluorescent dye yields the fluorescent, oxidized R6G, which localizes to the mitochondria.

Immunocytochemistry of HSCs

Immunocytochemistry of cytospun and PFA-fixed GFP^+ or YFP^+ virus–infected KLS cells was done as described previously (Kitsos *et al.*, 2005) using anti-$p27^{kip1}$, anti-$p21^{cip1}$, anti-Jab1 (all 1:100, Rabbit polyclonal; Santa Cruz Biotechnology, Santa Cruz, CA) and anti-Gfer (1:100, rabbit polyclonal; PTG Labs, Chicago, IL) primary antibodies. Cy3-conjugated secondary antibody (Jackson ImmunoResearch, West Grove, PA) was used, and samples were mounted using VECTASHIELD Mounting Medium with DAPI (4′,6-diamidino-2-phenylindole) (Vector Laboratories, Burlingame,

CA). Cells were observed using a fluorescence Axio Observer Z1 microscope with ApoTome assembly (Carl Zeiss, Thornwood, NY), and digital optical slice images were captured at 630× magnification. The signal intensities were calculated using AxioVision 2.0 software (Carl Zeiss) and analyzed on a Microsoft Excel (Redmond, WA) spreadsheet. For relevant experiments, KLS cells were treated for 1 h with 10 μM MG132 (Calbiochem, EMD Chemicals, Gibbstown, NJ), cytospun immediately thereafter, and fixed in 1% PFA for immunocytochemistry.

IP and immunoblot assays

Approximately 2 million EML cells were infected with MSCV-C, MSCV-Gfer, FG12 LacZ, and/or FG12 Gfer viruses and sorted for GFP expression 72 h later. Equal numbers of cells were lysed with Tween lysis buffer (Sankar *et al.*, 2004), sonicated, and precleared with protein A sepharose (GE Healthcare, Piscataway, NJ). Approximately 500 μg of whole-cell lysates were incubated with anti-$p27^{kip1}$ or anti-Jab1 antibodies (both mouse monoclonal; Santa Cruz Biotechnology) for 2 h at 4°C, and the IP complexes were captured using protein A Sepharose beads. The IP complexes were separated on SDS–PAGE and transferred to Immobilon polyvinylidine fluoride membrane (Millipore). Immunoblots were subsequently probed with rabbit polyclonal antibodies against $p27^{kip1}$, Jab1, ubiquitin (all obtained from Santa Cruz Biotechnology), and Gfer (PTG Labs). Signal intensities of bands were quantified using ImageQuant Capture Software (GE Healthcare) and analyzed using spread sheets.

Real-time reverse transcriptase PCR analysis

Total RNA was prepared from isolated HSCs using the RNAqueous-Micro and RNAqueous kits, respectively (Ambion, Austin, TX), according to the manufacturer's instructions. The first-strand cDNA was prepared using SuperScript III Reverse Transcriptase (Invitrogen) or High Capacity cDNA Reverse Transcription Kit (Applied Biosystems, Foster City, CA), according to the manufacturer's directions. Quantitative real-time PCR-based gene expression analysis was performed using IQ SYBR Green Supermix (BioRad Laboratories, Hercules CA) with the respective primers, and the reactions were performed using an IQ5 I-Cycler System (BioRad Laboratories). Gfer and actin primer sequences were previously mentioned (Todd *et al.*, 2010a).

Electron microscopy

Approximately 20,000 freshly resorted KLS cells were washed with PBS and pelleted. This cell pellet was then fixed in 3% glutaraldehyde in 0.1 M sodium cacodylate overnight at 4°C and post fixed in 1% osmium tetroxide in 0.1 M sodium cacodylate for 1 h. Cells were briefly rinsed with 0.1 M sodium cacodylate and then dehydrated using a series of graded alcohols embedded in LX-112 epoxy resin (Ladd Research Industries, Burlington, VT), and ~8 μm sections were cut on an LKB microtome (LKB Instruments, Gaithersburg, MD). Sections were then stained using uradyl acetate and lead citrate before viewing on a Phillips CM12 electron microscope (Phillips Electronic Instruments, Mahwah, NJ) equipped with a digital camera.

ACKNOWLEDGMENTS

We thank Michael Cook and Beth Harvat for help with flow cytometry; Jennifer Cates, Tyler Blythe, Elizabeth MacDougal, and Charles Mena for technical assistance; and the members of the Means and Sankar laboratories for discussions. This work was supported by a National Institutes of Health RO1 research grant (DK 074701; to A.R.M.), an American Cancer Society Postdoctoral Fellowship (PF-05–171-01-LIB), and funds from the James Graham Brown Cancer Center (to U.S.).

REFERENCES

Becher D, Kricke J, Stein G, Lisowsky T (1999). A mutant for the yeast scERV1 gene displays a new defect in mitochondrial morphology and distribution. Yeast 15, 1171–1181.

Bystrykh L *et al.* (2005). Uncovering regulatory pathways that affect hematopoietic stem cell function using "genetical genomics." Nat Genet 37, 225–232.

Cheng T, Rodrigues N, Dombkowski D, Stier S, Scadden DT (2000a). Stem cell repopulation efficiency but not pool size is governed by p27(kip1). Nat Med 6, 1235–1240.

Cheng T, Rodrigues N, Shen H, Yang Y, Dombkowski D, Sykes M, Scadden DT (2000b). Hematopoietic stem cell quiescence maintained by p21cip1/waf1. Science 287, 1804–1808.

Cheng T, Scadden DT (2002). Cell cycle entry of hematopoietic stem and progenitor cells controlled by distinct cyclin-dependent kinase inhibitors. Int J Hematol 75, 460–465.

Cheshier SH, Morrison SJ, Liao X, Weissman IL (1999). In vivo proliferation and cell cycle kinetics of long-term self-renewing hematopoietic stem cells. Proc Natl Acad Sci USA 96, 3120–3125.

DiMascio L, Voermans C, Uqoezwa M, Duncan A, Lu D, Wu J, Sankar U, Reya T (2007). Identification of adiponectin as a novel hemopoietic stem cell growth factor. J Immunol 178, 3511–3520.

Gatzidou E, Kouraklis G, Theocharis S (2006). Insights on augmenter of liver regeneration cloning and function. World J Gastroenterol 12, 4951–4958.

Ito K *et al.* (2004). Regulation of oxidative stress by ATM is required for self-renewal of haematopoietic stem cells. Nature 431, 997–1002.

Ito K *et al.* (2006). Reactive oxygen species act through p38 MAPK to limit the lifespan of hematopoietic stem cells. Nat Med 12, 446–451.

Ivanova NB, Dimos JT, Schaniel C, Hackney JA, Moore KA, Lemischka IR (2002). A stem cell molecular signature. Science 298, 601–604.

Kato JY, Yoneda-Kato N (2009). Mammalian COP9 signalosome. Genes Cells 14, 1209–1225.

Kitsos CM, Sankar U, Illario M, Colomer-Font JM, Duncan AW, Ribar TJ, Reya T, Means AR (2005). Calmodulin-dependent protein kinase IV regulates hematopoietic stem cell maintenance. J Biol Chem 280, 33101–33108.

Klebes A, Sustar A, Kechris K, Li H, Schubiger G, Kornberg TB (2005). Regulation of cellular plasticity in Drosophila imaginal disc cells by the Polycomb group, trithorax group and lama genes. Development 132, 3753–3765.

Klissenbauer M, Winters S, Heinlein UA, Lisowsky T (2002). Accumulation of the mitochondrial form of the sulphydryl oxidase Erv1p/Alrp during the early stages of spermatogenesis. J Exp Biol 205, 1979–1986.

Lange H, Lisowsky T, Gerber J, Muhlenhoff U, Kispal G, Lill R (2001). An essential function of the mitochondrial sulfhydryl oxidase Erv1p/ALR in the maturation of cytosolic Fe/S proteins. EMBO Rep 2, 715–720.

Lisowsky T, Lee JE, Polimeno L, Francavilla A, Hofhaus G (2001). Mammalian augmenter of liver regeneration protein is a sulfhydryl oxidase. Dig Liver Dis 33, 173–180.

Lu C *et al.* (2002). Intracrine hepatopoietin potentiates AP-1 activity through JAB1 independent of MAPK pathway. FASEB J 16, 90–92.

Mantel C, Messina-Graham S, Broxmeyer HE (2010). Upregulation of nascent mitochondrial biogenesis in mouse hematopoietic stem cells parallels upregulation of CD34 and loss of pluripotency: A potential strategy for reducing oxidative risk in stem cells. Cell Cycle 9, 2008–2017.

Mesecke N, Terziyska N, Kozany C, Baumann F, Neupert W, Hell K, Herrmann JM (2005). A disulfide relay system in the intermembrane space of mitochondria that mediates protein import. Cell 121, 1059–1069.

Miyamoto K *et al.* (2007). Foxo3a is essential for maintenance of the hematopoietic stem cell pool. Cell Stem Cell 1, 101–112.

Mori M, Yoneda-Kato N, Yoshida A, Kato J-y (2008). Stable form of JAB1 enhances proliferation and maintenance of hematopoietic progenitors. J Biol Chem 283, 29011–29021.

Morrison SJ, Wandycz AM, Hemmati HD, Wright DE, Weissman IL (1997). Identification of a lineage of multipotent hematopoietic progenitors. Development 124, 1929–1939.

Orford KW, Scadden DT (2008). Deconstructing stem cell self-renewal: genetic insights into cell-cycle regulation. Nat Rev Genet 9, 115–128.

Park IK, Qian D, Kiel M, Becker MW, Pihalja M, Weissman IL, Morrison SJ, Clarke MF (2003). Bmi-1 is required for maintenance of adult self-renewing haematopoietic stem cells. Nature 423, 302–305.

Polimeno L, Lisowsky T, Francavilla A (1999). From yeast to man–from mitochondria to liver regeneration: a new essential gene family. Ital J Gastroenterol Hepatol 31, 494–500.

Qin XF, An DS, Chen IS, Baltimore D (2003). Inhibiting HIV-1 infection in human T cells by lentiviral-mediated delivery of small interfering RNA against CCR5. Proc Natl Acad Sci USA 100, 183–188.

Ramalho-Santos M, Yoon S, Matsuzaki Y, Mulligan RC, Melton DA (2002). "Stemness": transcriptional profiling of embryonic and adult stem cells. Science 298, 597–600.

Sankar U, Patel K, Rosol TJ, Ostrowski MC (2004). RANKL coordinates cell cycle withdrawal and differentiation in osteoclasts through the cyclin-dependent kinase inhibitors p27KIP1 and p21CIP1. J Bone Miner Res 19, 1339–1348.

Schwechheimer C, Isono E (2010). The COP9 signalosome and its role in plant development. Eur J Cell Biol 89, 157–162.

Todd LR, Damin MN, Gomathinayagam R, Horn SR, Means AR, Sankar U (2010a). Growth factor erv1-like modulates Drp1 to preserve mitochondrial dynamics and function in mouse embryonic stem cells. Mol Biol Cell 21, 1225–1236.

Todd LR, Gomathinayagam R, Sankar U (2010b). A novel Gfer-Drp1 link in preserving mitochondrial dynamics and function in pluripotent stem cells. Autophagy 6, 821–822.

Tomoda K, Kato Jy, Tatsumi E, Takahashi T, Matsuo Y, Yoneda-Kato N (2005). The Jab1/COP9 signalosome subcomplex is a downstream mediator of Bcr-Abl kinase activity and facilitates cell-cycle progression. Blood 105, 775–783.

Tomoda K, Kubota Y, Arata Y, Mori S, Maeda M, Tanaka T, Yoshida M, Yoneda-Kato N, Kato JY (2002). The cytoplasmic shuttling and subsequent degradation of p27Kip1 mediated by Jab1/CSN5 and the COP9 signalosome complex. J Biol Chem 277, 2302–2310.

Tomoda K, Kubota Y, Kato Jy (1999). Degradation of the cyclin-dependent-kinase inhibitor p27Kip1 is instigated by Jab1. Nature 398, 160–165.

Tsai S, Bartelmez S, Sitnicka E, Collins S (1994). Lymphohematopoietic progenitors immortalized by a retroviral vector harboring a dominant-negative retinoic acid receptor can recapitulate lymphoid, myeloid, and erythroid development. Genes Dev 8, 2831–2841.

Viatour P, Somervaille TC, Venkatasubrahmanyam S, Kogan S, McLaughlin ME, Weissman IL, Butte AJ, Passegue E, Sage J (2008). Hematopoietic stem cell quiescence is maintained by compound contributions of the retinoblastoma gene family. Cell Stem Cell 3, 416–428.

Wang Y, Lu C, Wei H, Wang N, Chen X, Zhang L, Zhai Y, Zhu Y, Lu Y, He F (2004). Hepatopoietin interacts directly with COP9 signalosome and regulates AP-1 activity. FEBS Lett 572, 85–91.

Wei N, Serino G, Deng XW (2008). The COP9 signalosome: more than a protease. Trends Biochem Sci 33, 592–600.

Wilson A *et al*. (2008). Hematopoietic stem cells reversibly switch from dormancy to self-renewal during homeostasis and repair. Cell 135, 1118–1129.

Wilson A, Trumpp A (2006). Bone-marrow haematopoietic-stem-cell niches. Nat Rev Immunol 6, 93–106.

Yalcin S, Zhang X, Luciano JP, Mungamuri SK, Marinkovic D, Vercherat C, Sarkar A, Grisotto M, Taneja R, Ghaffari S (2008). Foxo3 is essential for the regulation of ataxia telangiectasia mutated and oxidative stress-mediated homeostasis of hematopoietic stem cells. J Biol Chem 283, 25692–25705.

Yilmaz OH, Valdez R, Theisen BK, Guo W, Ferguson DO, Wu H, Morrison SJ (2006). Pten dependence distinguishes haematopoietic stem cells from leukaemia-initiating cells. Nature 441, 475–482.

Zhou W, Yang Q, Low CB, Karthik BC, Wang Y, Ryo A, Yao SQ, Yang D, Liou YC (2009). Pin1 catalyzes conformational changes of Thr-187 in p27Kip1 and mediates its stability through a polyubiquitination process. J Biol Chem 284, 23980–23988.